Vaccine 42 (2024) 2895–2908

Contents lists available at ScienceDirect

Vaccine

journal homepage: www.elsevier.com/locate/vaccine

Evaluation of bird-adapted self-amplifying mRNA vaccine formulations in chickens

Jerome D.G. Comes [a], Kristel Doets [a,b], Thijmen Zegers [a], Merel Kessler [a], Irene Slits [a], Natalia A. Ballesteros [b], Noortje M.P. van de Weem [b], Henk Pouwels [b], Monique M. van Oers [a], Marielle C.W. van Hulten [b], Martijn Langereis [b], Gorben P. Pijlman [a,*]

[a] Laboratory of Virology, Wageningen University & Research, Droevendaalsesteeg 1, Wageningen 6708PB, the Netherlands
[b] MSD Animal Health, Wim de Körverstraat 35, Boxmeer 5831AN, the Netherlands

ARTICLE INFO

Keywords:
Duck Tembusu virus replicon
Self-amplifying mRNA
Lipid nanoparticles
Viral poultry diseases

ABSTRACT

Each year, millions of poultry succumb to highly pathogenic avian influenza A virus (AIV) and infectious bursal disease virus (IBDV) infections. Conventional vaccines based on inactivated or live-attenuated viruses are useful tools for disease prevention and control, yet, they often fall short in terms of safety, efficacy, and development times. Therefore, versatile vaccine platforms are crucial to protect poultry from emerging viral pathogens. Self-amplifying (replicon) RNA vaccines offer a well-defined and scalable option for the protection of both animals and humans. The best-studied replicon platform, based on the Venezuelan equine encephalitis virus (VEEV; family *Togaviridae*) TC-83 vaccine strain, however, displays limited efficacy in poultry, warranting the exploration of alternative, avian-adapted, replicon platforms. In this study, we engineered two Tembusu virus (TMUV; family *Flaviviridae*) replicons encoding varying capsid gene lengths and compared these to the benchmark VEEV replicon *in vitro*. The TMUV replicon system exhibited a robust and prolonged transgene expression compared to the VEEV replicon system in both avian and mammalian cells. Moreover, the TMUV replicon induced a lesser cytopathic effect compared to the VEEV replicon RNA *in vitro*. DNA-launched versions of the TMUV and VEEV replicons (DREP) were also developed. The replicons successfully expressed the AIV haemagglutinin (HA) glycoproteins and the IBDV capsid protein (pVP2). To assess the immune responses elicited by the TMUV replicon system in chickens, a prime-boost vaccination trial was conducted using lipid nanoparticle (LNP)-formulated replicon RNA and DREP encoding the viral (glyco)proteins of AIV or IBDV. Both TMUV and VEEV replicon RNAs were unable to induce a humoral response against AIV. However, TMUV replicon RNA induced IBDV-specific seroconversion in vaccinated chickens, in contrast to VEEV replicon RNA, which showed no significant humoral response. In both AIV and IBDV immunization studies, VEEV DREP generated the highest (neutralizing) antibody responses, which underscores the potential for self-amplifying mRNA vaccine technology to combat emerging poultry diseases.

1. Introduction

The development of new efficacious vaccine platforms is crucial to protect chickens against novel emerging viral pathogens that annually cause the death of millions of poultry worldwide. During the 1997 avian influenza virus (AIV) H5N1 pandemic, it became clear that solely human vaccination against zoonotic influenza viruses was not sufficient to prevent new pandemics from arising [1,51,54,57,66]. Since then, not only vaccination of poultry against AIV H5N1 was implemented, but also routine vaccination against other avian-specific pathogens gained more interest as a potent control measure to prevent disease worldwide [3,64]. Although conventional (inactivated or live-attenuated) vaccines were a step forward in the prevention and control of diseases in birds, the vaccines often performed sub-optimally in terms of safety, efficacy, or development times [34,63]. As such, millions of poultry are culled each year due to the sudden occurrence of highly pathogenic AIV or very virulent infectious bursal disease virus (IBDV). To mitigate morbidity, mortality, and the zoonotic spillover of poultry pathogens to humans, an effective and versatile vaccine platform technology is required.

Conventional vaccines are less suitable for emergency vaccination

* Corresponding author.
E-mail address: gorben.pijlman@wur.nl (G.P. Pijlman).

https://doi.org/10.1016/j.vaccine.2024.03.032
Received 6 November 2023; Received in revised form 11 March 2024; Accepted 13 March 2024
Available online 23 March 2024

during an outbreak, because of biosafety regulations, difficulties during pathogen cultivation, or less control over batch-to-batch variations. The first step in creating a more easily adaptable vaccine platform was the registration of recombinant live viral vector vaccines. A commercially available vector for poultry is the genetically modified version of the Meleagrid herpesvirus 1, commonly known as Turkey herpesvirus or Herpesvirus of Turkey (HVT). This recombinant HVT vaccine can be modified relatively easily and can encode multiple antigens of interest rendering it a suitable platform for multivalent vaccination [31,32,56,58]. Nevertheless, scaling up the production of this cell-associated recombinant live virus is challenging due to the requirement of primary chicken embryo fibroblast cells for virus propagation, which restricts its suitability as a platform for rapid response vaccines [52,65].

Interestingly, the recent COVID-19 pandemic has accelerated the use of nucleic acid-based messenger (m)RNA vaccines, which are also attractive for the poultry industry as they are generally well-defined, scalable, and most importantly, quickly adaptable. Current mRNA vaccines for human use require a substantial dose (30 μg for BioNtech/Pfizer's Comirnaty, 100 μg for Moderna's Spikevax) plus a booster vaccination in order to provide protective immunity [17,41]. However, smaller doses have been reported for self-amplifying mRNA (samRNA or SAM) vaccines, the so-called replicons [2]. These replicon formulations are often based on the replication genes of Venezuelan equine encephalitis virus (VEEV; family *Togaviridae;* genus *Alphavirus)* TC-83 vaccine strain or Kunjin virus (KUNV; family *Flaviviridae,* genus *Flavivirus*) [29,46]; R. [59,61]. To generate replicon vaccines, the wildtype viral genome is modified by replacing the viral structural genes for a gene of interest. Since only the replicase genes are maintained, the replicon RNA can self-amplify in the cytoplasm but cannot propagate or spread to other cells. The process of active RNA amplification in cells receiving the replicon may eliminate the need for an adjuvant while a strong immune response is induced [9,29,60]. Immune responses targeting the replicase genes may also be induced, but this does not negatively impact repeated vaccinations with the same replicon vector [46]. Despite this self-adjuvating effect of replicon vaccines, the VEEV replicon platform does not always induce a protective immune response in poultry [50,55]. Consequently, there is a niche for an alternative, preferably poultry-adapted, replicon-based platform. A suitable virus candidate to develop an alternative replicon for poultry is the Tembusu virus (TMUV), a member of the *Flaviviridae* family. TMUV has been isolated from a wide range of bird species such as ducks, geese, chickens, and pigeons, and thus shares hosts with the avian influenza virus [15].

In this study, we describe the construction of modified TMUV replicons containing an extended capsid-coding region comprising conserved secondary RNA structures. Additionally, we demonstrate the effect of these *cis*-acting elements within the capsid gene on the expression levels, duration, and cytopathic effect in comparison to the VEEV replicon benchmark. Furthermore, we describe the immunization of chickens with TMUV- versus VEEV-based replicons containing the viral structural transgenes of AIV (HA) or IBDV (pVP2). We further developed a DREP platform based on the Tembusu Perak isolate and compared this construct to a VEEV DREP construct. Replicon RNA or DREP vectors were formulated in lipid nanoparticles (LNP) and administered in a homologous prime-boost setting to 1-day-old specific-pathogen-free (SPF) chickens. The humoral responses in chickens against HA and VP2 were followed over time for all vaccine candidates and compared to those induced by a commercial vaccine. We conclude that a synthetically-produced, TMUV-based replicon system has the potential to vaccinate poultry against emerging viral pathogens.

2. Material and methods

2.1. Cells

Baby hamster kidney cells (BHK-21; CCL-10) and chicken embryonic fibroblast cells (DF-1; CRL-3586) were cultured at 37 °C under 5 % CO_2 in Dulbecco's modified Eagle's medium (DMEM; Gibco) supplemented with 10 % fetal bovine serum (FBS) and 100 U/mL penicillin–streptomycin (Gibco).

2.2. Plasmids

TMUVrep-C_{20} and VEEV replicons (Fig. 1A,) have been described (Comes et al., 2024) [5]. The constructed TMUV DREP was based on the duck Tembusu Perak isolate (Genbank accession no.: KX097989) and synthesized in a single-copy pCC1BAC backbone (Genscript)(Fig. 3A). VEEV DREP was based on the attenuated VEEV TC-83 strain and synthesized in a high-copy pUC57 backbone (Genscript) [21,29]. Both DREP constructs were designed with the cytomegalovirus (CMV) promoter upstream of the replicon sequence. To ensure the formation of a native 3′ untranslated region (UTR) in the TMUV replicon RNA, similar to that described in (Comes et al., 2024) [5], a hepatitis delta virus (HDV) ribozyme and simian virus 40 (SV40)-poly(A) signal were included downstream of the 3′UTR terminus. To insert the viral transgenes of HA (AIV) or pVP2 (IBDV) in the TMUV and VEEV DREP, unique *AscI-AvrII* and *AscI-PacI* restriction sites were incorporated in each replicon, respectively. For the construction of TMUVrep-C_{38}-eGFP, the first 20 codons of the capsid coding region of TMUVrep-C_{20}-eGFP replicon construct were replaced via restriction digestion (*KasI* and *AscI*) by a synthetic DNA gene (Thermo Fisher Scientific) coding for the first 38 codons of the capsid gene [5] (Fig. 2A). All plasmids were purified using the endotoxin-free Nucleobond Midiprep kit (Macherey-Nagel) and the DNA concentration was determined using the spectrophotometer ND-1000 (Nanodrop). Plasmids were stored for further use at −80 °C. For the evaluation of TMUV and VEEV DREP constructs, subconfluent (60–70 % confluency) BHK-21 cells in 6-wells plates were transfected with 2 micrograms using Lipofectamine 2000 reagent (Invitrogen) in Opti-MEM (Gibco) according to the manufacturer's protocol. After 4 h, the monolayer was washed with Dulbecco's phosphate-buffered saline (DPBS; Gibco), and fresh supplemented medium was added. Cells were incubated at 37 °C under 5 % CO_2 prior to indirect immunofluorescence assays.

2.3. Secondary RNA structure prediction

Models of the secondary RNA structures within the 5′UTR and capsid region of the TMUV WU2016 genome (Genbank accession no.: OQ920272) were predicted using the webserver RNAalifold (http://rna.tbi.univie.ac.at/cgi-bin/RNAWebSuite/RNAalifold.cgi) and RNAstructure 6.3 and verified using the phylogenetically related TMUV isolates aligned in Clustal X V2.0. The secondary RNA structures were visualized and modeled in VARNA [8]. The secondary structures that were selected are based on the minimum free energy prediction not taking into account weaker GU pairs at the end of helices. For long-distance RNA interaction such as 5′ upstream AUG region (5′UAR), 5′ downstream AUG region (5′DAR), and 5′ cyclization signal (5′CS) the prediction was generated using the Mfold web server in which the 5′UTR and 3′UTR were separated by a poly(A) stretch of 100 nt [26].

2.4. In vitro replicon RNA transcription, purification, and electroporation

The construction of the SP6-driven TMUVrep-C_{20} replicon, encoding the first 20 N-terminal amino acids of the capsid protein, has been described in Comes et al. (2024) [5]. A similar approach was applied for the construction of SP6/T7-driven TMUVrep-C_{38} and VEEVrep expressing various reporter and viral (glyco)proteins. Replicon-encoding DNA plasmids were purified using the endotoxin-free Nucleobond Midiprep kit (Macherey-Nagel) and linearized using *PacI* (TMUV-derived replicons) or *NotI* (VEEV-derived replicons) restriction enzymes. Capped *in vitro* transcribed replicon RNAs were generated by using 2.5 micrograms of linearized plasmid DNA in an SP6- or a T7-polymerase

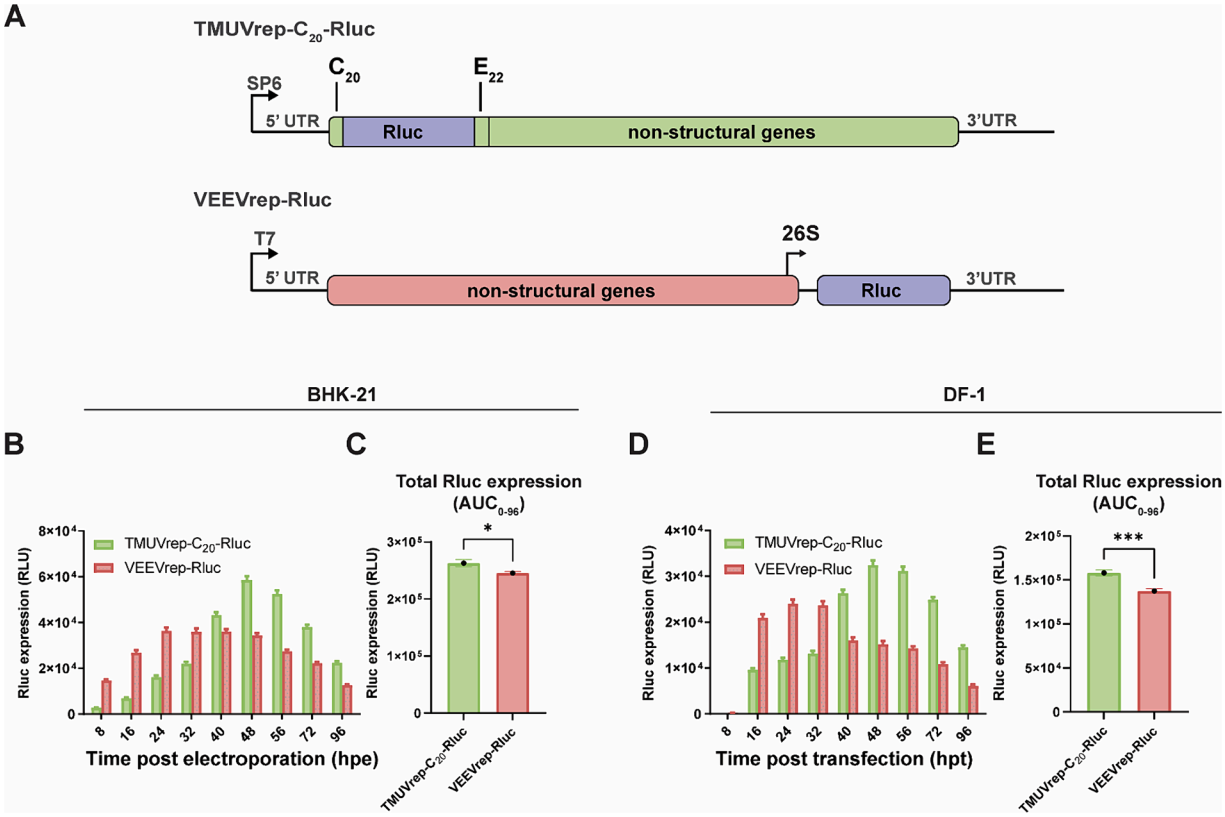

Fig. 1. Comparison of Rluc expression between the TMUV and VEEV replicon RNA in mammalian and avian cell lines. (A) Schematic diagram of the SP6 promoter-driven TMUV replicon construct and T7 promoter-driven VEEV replicon construct encoding the Rluc protein. C20: first 20 amino acids of capsid; E22: last 22 amino acids of envelope protein; 26S: 26S promoter are indicated. Rluc activity expressed in RLU of TMUVrep-C_{20}-Rluc or VEEVrep-Rluc electroporated (B) BHK-21 cells or transfected (D) DF-1 cells over 96-hour period. (C & E) The total (0–96 h) Rluc expression was calculated by approximating the area under the curve ($AUC_{0\text{-}96}$) by dividing it into trapezoids and summing their areas. Two independent experiments are presented as means and SEM, with significance defined by $p \leq 0.05$ (*) and $p \leq 0.0005$ *(***)* in an unpaired Student's *t*-test. hpe = hours post electroporation, hpt = hours post transfection.

reaction (both from New England Biolabs) for TMUV and VEEV replicon constructs, respectively. The reactions were incubated for 2 h at 37 °C and thereafter treated for 30 min at 37 °C with RNAse-free DNAse (Promega). Replicon RNA was purified using the RNeasy Midiprep kit (Qiagen) according to the manufacturer's RNA Cleanup protocol. Both quantity and quality of the *in vitro* transcribed RNA was analyzed using spectrophotometry (ND-1000; Nanodrop) and via conventional electrophoresis using a 1 % agarose gel in tris–acetate-EDTA (TAE) buffer for 15 min at 150 V. The generated replicon RNA was stored at −80 °C until further use. For the evaluation of replicon RNA, BHK-21 cells were electroporated using the Gene Pulser Xcell (Bio-Rad Laboratories). Purified replicon RNA was mixed with 6×10^6 resuspended BHK-21 cells in DPBS and pulsed twice (850 V/25µF) in a 0.4 cm electroporation cuvette (Bio-Rad Laboratories). After electroporation, cells were recovered in 10 mL supplemented medium and incubated at 37 °C under 5 % CO_2.

2.5. Renilla luciferase activity assay

To assess the Renilla luciferase (Rluc) activity, 24-well plates were seeded with 1 x 10^5 cells/well of electroporated BHK-21 or transfected DF-1 cells containing TMUVrep-C_{20}-Rluc or VEEVrep-Rluc replicon RNA and incubated up to 4 days. At various time points, the cells were lysed using a passive lysis buffer (Promega) for 20 min at RT. The cell lysate was cleared using centrifugation at 12.000×*g* and transferred into an opaque 96-well plate. Next, pre-made Rluc buffer was mechanically injected using the FLUOstar Optima microplate reader (BMG Labtech). The luminescence was measured in triplicate for 8 min (10 intervals) and normalized against mock electroporated BHK-21 cells. To determine the total expression, which represents the area under the curve (AUC), values were processed using the trapezoid rule. Student's *t*-test was performed using GraphPad Prism (V9.5.0.) to assess the statistical significance ($p \leq 0.05$ was considered statistically significant).

2.6. Viral cytotoxicity assay

To assess the cytopathic effect (CPE) of the TMUV and VEEV replicon RNA on BHK-21 cells, 1.5×10^4 electroporated cells/well were plated in a 96-well plate (Greiner). The cells were analyzed every 24 h up to 4 days post electroporation to evaluate the CPE using the Viral ToxGlo assay (Promega) according to the manufacturer's protocol. The luminescence was measured using the FLUOstar OPTIMA microplate reader (BMG Labtech). The virus-induced cytotoxicity was determined by the average RLU of two biological and three technical replicates normalized against the average RLU of healthy, mock electroporated cells.

2.7. Flow cytometry analysis

eGFP or wrmScarlet expression were measured using the SH800S Cell sorter (Sony) or Accuri C6 (BD Biosciences), respectively. For flow cytometry analysis, cells were collected via trypsinization, washed with DPBS, and resuspended in FACS buffer (DPBS supplemented with 1 % BSA and 1 mM EDTA). Forward scatter (FSC) and back/side scatter (BSC/SSC) were used to exclude debris, abnormalities, and doublets. To determine the mean fluorescence intensity (MFI) of the highest 5 % of GFP-positive cells, a standard gating strategy was implemented that excluded 99 % of non-fluorescent mock cells. A total of 100.000 events per sample were measured.

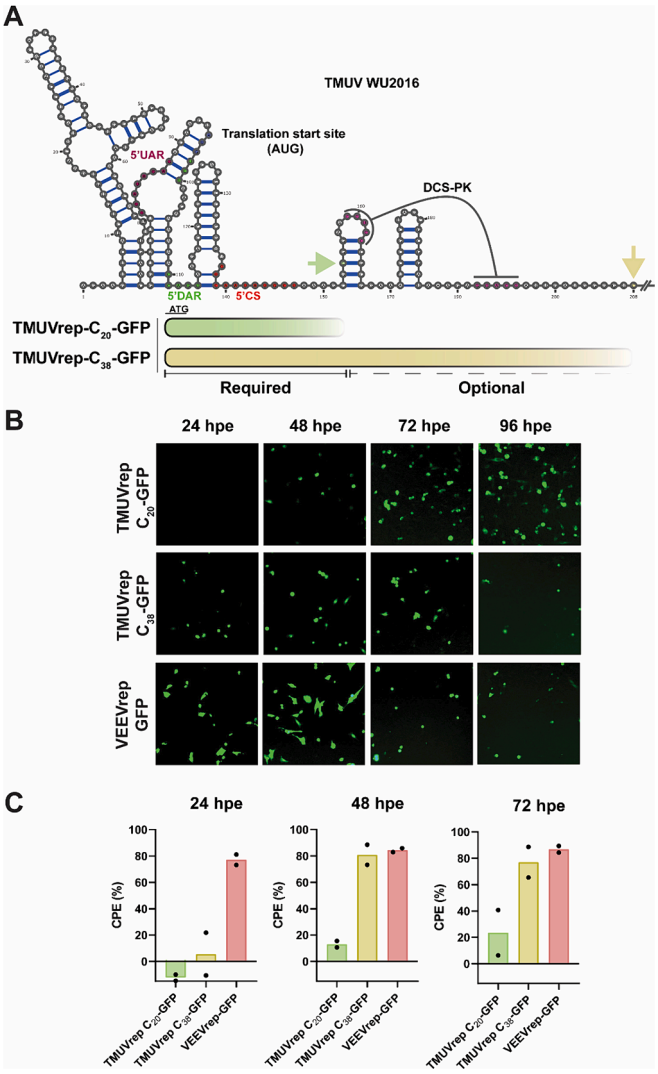

Fig. 2. The effect of *cis*-acting elements encoded within capsid gene on the heterologous protein expression and cytopathicity of the TMUV replicon. (A) Prediction of conserved secondary RNA structures using RNAstructure 6.3 and RNAalifold amongst different TMUV isolates within the first 208 nt of the capsid gene. Secondary structures were drawn using RNAalifold and VARNA software package [8]. The following *cis*-acting elements were identified: 5′ upstream of AUG region (5′UAR), 5′ downstream of AUG region (5′DAR), 5′ cyclization sequence (5′CS), and downstream of 5′CS pseudoknot (DCS-PK). Two different TMUV replicon RNAs were constructed to encode the first 20 (C_{20}) or 38 (C_{38}) amino acids of the capsid protein. (B) Fluorescence images of BHK-21 cells electroporated with TMUVrep-C_{20}-GFP, TMUVrep-C_{38}-GFP, and VEEVrep-GFP replicon RNA over a time period of 96-hours. (C) A comparative cytopathic effect analysis (Viral ToxGlo assay) was performed based on cellular ATP as a surrogate marker of host cell viability of BHK-21 cells harbouring TMUVrep-C_{20}-GFP, TMUVrep-C_{38}-GFP and VEEVrep-GFP at 24, 48 and 72 h post electroporation (hpe).

2.8. Replicon formulation into lipid nanoparticles

The purified replicon RNA and DNA-encoded replicon plasmids were formulated into LNPs. First, a mixture of ionizable lipids, cholesterol, distearoylphosphatidylcholine (DSCP), and polyethylene glycol (PEG) C14 was dissolved at a molar ratio of 58:30:10:2 to a final lipid concentration of 22.34 mM in absolute ethanol. The lipid mixture was then emulsified (N/P ratio 6) with a citrate buffer (pH 5) containing the purified DNA or RNA stock using the NanoAssemblr microfluidic system (Precision Nanosystems). Next, the resulting LNPs were dialyzed against ddH_2O for 3–6 h at RT and subsequently against TRIS-G buffer (10 mM TRIS, 70 mM NaCl, 5 % sucrose) for 12–18 h at 2–8 °C. The dialyzed LNPs were then filter sterilized using a double-layer filter (Acrodisc PF syringe filter, 0.8/0.2 μm/25 mm; Thermofisher Scientific). Following this, the LNP particle size (Z-average) and polydispersity (pdi) were measured by dynamic light scattering (DLS, Zetasizer APS2000, Malvern). The LNPs were analyzed by transmission electron microscopy. Briefly, LNPs were loaded onto 200-mesh carbon-coated copper grids (Electron Microscopy Sciences, Hatfield, PA, USA) and stained with 2 % ammonium molybdate. Grids were analyzed using a JEOL JEM-1400Plus transmission electron microscope. The concentration and formulation efficiency was determined by an LNP disruption assay specific for either DNA or RNA. For the DNA:LNP disruption assay, 10 μL of each DNA:LNP formulation was treated using 4 % (v/v) Triton-X-100 in DPBS and incubated at 37 °C for 10 min. Hereafter, the disrupted LNPs were mixed with 0.2 % SybrGold in DPBS solution, and incubated for 60 sec. while agitating at 500 rpm and measured using the ClarioStar spectrofluorometer (ex.: 485 nm, em.: 530 nm; BMG Labtech). A plasmid DNA standard was used to determine the DNA concentration. For the RNA:LNP disruption assay, 10 μL of each RNA:LNP formulation was treated using 4 % (v/v) Triton-X-100 in DEPC-treated ddH_2O and incubated at 37 °C for 10 min. The released RNA was separated using conventional gel-electrophoresis (1 % agarose in TAE buffer) for 30 min at 150 V. Quantitative and qualitative analysis of the released RNA was accomplished using an in-house replicon RNA standard and Image Lab software (Bio-Rad Laboratories).

2.9. Coomassie brilliant blue staining and western blotting

Cell fractions and precipitated supernatant fractions were dissolved in DPBS and incubated at 95 °C for 5–10 min with a loading buffer containing β-mercaptoethanol. Protein samples were then separated using an 8–16 % Mini-PROTEAN TGX Precast Protein gel (Bio-Rad Laboratories). After electrophoresis, proteins were visualized by Coomassie brilliant blue (CBB) staining or transferred to a polyvinylidene difluoride membrane (PVDF; Invitrogen) for immunodetection. Membranes were blocked overnight at 4 °C with 5–10 mL DPBS-T containing 1 % skimmed milk (blocking buffer). Then, membranes were incubated for 1 h at room temperature with diluted convalescent α-HA serum (chicken, 1:500) or α-VP2 (mouse, R63) [53] antibodies in blocking buffer. Thereafter, secondary antibodies α-chicken IgY-alkaline phosphatase (AP; goat, 1:2500; Sigma-Aldrich) or α-mouse IgG-AP (goat, 1:2500; Sigma-Aldrich) were added and incubated for 1 h at RT. Membranes were washed and proteins were visualized by incubation with 5-bromo-4-chloro-3-indolyl phosphate (NBT/BCIP; Sigma-Aldrich) in 5 mL AP buffer. To remove the *N*-glycosylated groups from the glycoproteins, cell lysates were treated using peptide-N-glycosidase F (PNGase F; New England Biolabs) according to the manufacturer's recommendation.

2.10. Indirect immunofluorescence assay

Indirect immunofluorescence assays were performed to detect the presence of viral (glyco)proteins in replicon-transfected cells. The monolayer of BHK-21 cells were washed using DPBS and fixed using 4 % paraformaldehyde in DPBS at RT for 5 min. The cells were washed and permeabilized using 0.1 % sodium dodecyl sulfate (SDS) in DPBS at RT for 10 min. Next, the monolayer was blocked by 5 % FBS in DPBS at 37 °C for 1 h and incubated at 37 °C for 1 h with primary antibody diluted in 5 % FBS in DPBS; for α-VP2 (mouse, 1:1000), α-HA serum (chicken, 1:500). Hereafter, cells were incubated with a secondary α-mouse or α-chicken IgG conjugated with Alexa fluor 546 (goat, 1:2000; Invitrogen) antibody in 5 % FBS in DPBS at 37 °C for 1 h. Cells were then stained with Hoechst (1:100; Thermo Fisher Scientific,) in DPBS for 5 min. Photos were acquired using the Axio Observer Z1 fluorescence microscope (Zeiss).

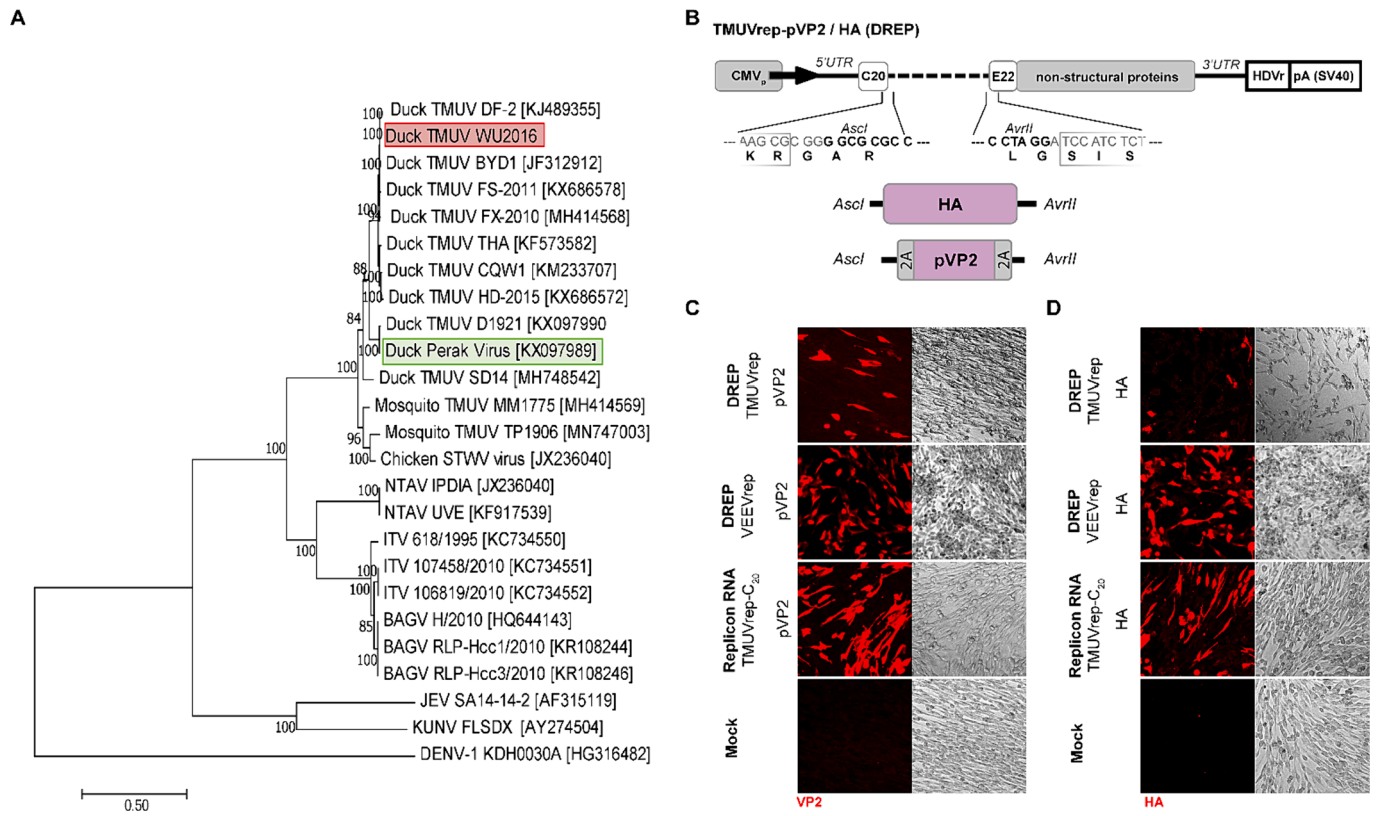

Fig. 3. Construction and validation of the TMUV DREP. (A) Phylogenetic analysis of the TMUV isolate Perak based on a multiple sequence alignment of the complete flavivirus genomes retrieved from Genbank. The tree was constructed using the maximum likelihood method based on the general time reversible model. A discrete gamma (+G) distribution was used to model evolutionary rate differences among sites. The tree with the highest likelihood is shown in which the percentage indicates the constructed trees were the included isolates clustered together (100 replicates) [28,43]). (B) Design of the TMUV Perak DREP is similar to the replicon RNA construct. The AscI and AvrII cloning sites (bold) within the DREP construct allow for in-frame insertion of the avian influenza virus haemagglutinin gene (HA) and infectious bursal disease virus nucleocapsid protein (pVP2) flanked by foot-and-mouth disease virus (FMDV) 2A elements. The RNA transcription is under control of the human cytomegalovirus promoter (CMV_p starting from the 5′ untranslated region (UTR). To ensure that the highly conserved 3′ untranslated region (UTR) contained an authentic nucleotide end, a Hepatitis δ virus-like ribozyme (HDVr) followed by the simian virus 40 (SV40) polyadenylation signal (pA) was inserted downstream of the last nucleotide of the 3′UTR. C20: first 20 amino acids of capsid; E22: last 22 amino acids of envelope protein are indicated. BHK-21 cells transfected with TMUV replicon RNA, TMUV DREP or VEEV DREP expressing the viral (glyco) proteins (C) pVP2 or (D) HA were detected using an indirect immunofluorescence assay. Primary antibodies: α-HA convalescent sera (chicken), monoclonal α-VP2 IgG (mouse). Secondary antibody: Alexa Fluor 546-conjugated α-chicken IgY (goat) or α-mouse IgG (goat).

2.11. Chicken vaccination and sampling

One-day-old, specific-pathogen-free (SPF) chickens (white leghorn layers) were divided into 5 groups (HA-vaccination trial) or 6 groups (VP2-vaccination trial) with 10 chickens in each group. The chickens assigned to each group were tagged and placed in a housing isolator with water and feed *ad libitum*. Day-old chickens were vaccinated via the intramuscular route with 10 µg or 3 µg LNP-formulated replicon RNA or DREP, respectively. At T = 3 weeks, an additional booster injection of 10 µg (LNP:RNA) or 3 µg (LNP:DREP) was administered. One-day-old chickens belonging to the positive control group were vaccinated subcutaneously in the neck with Innovax-ND-IBD (MSD Animal Health, Boxmeer). The mock group received no vaccination. Blood samples (1.1 mL) were collected from the left- and right-wing vein of all individuals in each group at t = 3, 5, 7, 10, and 13 weeks post-vaccination. Serum was collected using Bio-One Vacuette Z Serum clot activator tubes (Greiner). Clotting of the blood was achieved by inverting the tubes and incubation at 4 °C for 30 min. Subsequently, the tubes were centrifuged at 3.000 x g at 20 °C for 10 min and then heat-inactivated at 56 °C for 30 min. The serum samples were stored at −20 °C.

2.12. Serology

HA- and VP2-specific antibodies from the collected sera were detected with a commercially available antibody ELISA kit (ID Screen Influenza H5 indirect or ID Screen IBD VP2; IDvet) or reversed competition ELISA kit (IDscreen Influenza H5 antibody competition; IDvet) according to the standard protocol described by the manufacturer. Hemagglutination inhibition (HI) assays were used for the HA serotype-specific detection of antibodies against the H5N1 subtype according to the World Health Organization guidelines (World Health Organization, 2002). An unpaired, two-tailed *t*-test (Mann-Whitney) was used to assess the statistical significance of the antibody readouts detected in the indirect ELISAs and HI assays ($p \leq 0.05$ was considered statistically significant). Serological responses to IBDV were tested using a virus neutralization test using IBDV strain D78 and chicken embryonic cells as described previously [49]. Titres of ≥ 4 1og2 were considered to be positive.

3. Results

3.1. Comparison of reporter transgene expression between TMUV replicon RNA and VEEV replicon RNA

Previously, a TMUV replicon was constructed based on the TMUV WU2016 infectious cDNA clone[5]. To compare the expression kinetics of the TMUV replicon to the benchmark VEEV replicon in mammalian and avian cell lines, both replicon RNAs were modified to express the

Rluc protein (Fig. 1A). Replicon RNA was electroporated into BHK-21 cells or transfected into DF-1 cells, which were sampled over multiple time points in a 96-hours period to quantify the Rluc activity as a measure of gene expression (Fig. 1B and 1D). It was observed that the VEEV replicon RNA resulted in an early onset (8 hpe in BHK-21 cells and 8 hpt for DF-1 cells) of Rluc expression while the TMUV-mediated expression was lower at these earlier time points in BHK-21 (Fig. 1B) and DF-1 (Fig. 1D). Despite the later onset of Rluc expression by TMUV, the total Rluc activity over 96-hours period was significantly higher than VEEV replicon RNA expressed Rluc in BHK-21 (Fig. 1C) and in DF-1 cells (Fig. 1E).

In earlier studies, the functional flexibility of the TMUV virus capsid gene was evaluated, highlighting the consequences of including a truncated capsid-coding region and its positive implications of putative *cis*-acting elements on viral replication[18]. Structural analysis of the 5′ terminal region of the TMUV WU2016 RNA genome revealed the presence of secondary RNA structures within the 5′ UTR and the capsid gene (Fig. 2A). In order to investigate the role of these specific *cis*-acting elements on the dynamics of transgene expression from TMUV replicon RNA, an additional TMUV replicon was constructed that encodes the first 38 amino acid residues of the capsid protein (TMUVrep-C_{38}-GFP). The RNA of this region contains the secondary structure known as 'downstream of cyclization signal pseudoknot' (DCS-PK) [26]; Z.-Y. [33] (Fig. 2A). The impact of the DCS-PK on the expression kinetics and virus-induced cytotoxicity was evaluated by introducing TMUVrep-C_{20}-GFP, TMUVrep-C_{38}-GFP, and VEEVrep-GFP replicon RNA into BHK-21 cells through electroporation (Fig. 2B & C). Interestingly, the inclusion of DCS-PK in the replicon RNA (TMUVrep-C_{38}-GFP) resulted in the detection of GFP-expressing cells as early as 24 hpe, similar to VEEVrep-GFP (Fig. 2B). Although the onset of GFP expression differed between TMUVrep-C_{20}-GFP and TMUVrep-C_{38}-GFP, no noticeable difference in GFP accumulation was observed at later time points (Supplementary Fig. S1).

The effect of the DCS-PK also became apparent when comparing the virus-induced cytopathic effect (CPE) of the various replicon RNAs (Fig. 2C). No observable difference was detected between the TMUVrep-C_{20}-GFP and TMUVrep-C_{38}-GFP in the first 24 h, however, after 48 h a noticeably stronger CPE was seen for TMUVrep-C_{38}-GFP. In contrast, VEEVrep-GFP evidently showed more intense CPE from 24 h onwards, which was also apparent from the changes in cell morphology and the loss of fluorescent cells (Supplementary Fig. S2). Thus, the addition of the DCS-PK in the TMUV replicon RNA seems to increase replication efficiency which results in faster *trans*-gene expression and increased CPE.

3.2. Design and construction of a DNA-launched replicon construct

The design of the DREP was based on the duck Tembusu virus isolate Perak (Genbank accession nr: KX097989), which is a virus isolated from ducks[20]. TMUV Perak shows a high nucleotide (92 %) and protein (99 %) sequence identity to the previously described TMUV WU2016 (Genbank accession no.: OQ920272). Whole genome analysis shows that TMUV Perak clusters together with other duck-derived TMUV isolates (Fig. 3A). A more distant relationship is observed for mosquito and chicken-derived isolates such as TMUV MM1775 and Sitiawan virus (STWV), respectively.

For the TMUV DREP platform, the design contained only the first 20 amino acids of the capsid protein and the last 22 amino acids of the envelope protein (Fig. 3B), similar to the RNA replicon design[5]. The DREP constructs were transfected into BHK-21 cells and the expression of viral transgenes was visualized using an indirect immunofluorescence assay (Fig. 3C & D). The expression of pVP2 (Fig. 3C) and HA (Fig. 3D) from TMUV DREPs was detectable by IFA despite the lower transfection efficiency compared to the benchmark VEEV DREP or the TMUV replicon RNA. These differences in expression efficiency might be explained by the significantly larger size of the TMUV DREP (pCC1BAC, 11.6 kbp + TMUV replicon, ~10.5 kbp ≈ 22 kbp) compared to the VEEV DREP (pUC57, 3.1 kb + VEEV replicon ~9.5kbp ≈ 12.6 kbp).

3.3. Viral (glyco)protein translocation and glycosylation status

To investigate whether the viral (glyco)proteins expressed from the different replicons were correctly processed intracellularly, BHK-21 cells were transfected with replicon RNA of either the TMUVrep-C_{20}-pVP2, VEEVrep-pVP2, TMUVrep-C_{20}-HA, or VEEVrep-HA to determine the localization of the pVP2 and HA proteins. Since the pVP2 protein of wildtype IBDV is autoproteolytically processed in the cytoplasm [38], it is expected that pVP2 accumulates in a similar location when expressed from the replicon RNA (Fig. 4A). The AIV membrane protein HA naturally encodes both a signal sequence (SS) and a transmembrane domain (TMD) targeting the protein to the ER and subsequently via the Golgi to the plasma membrane (Fig. 4A). The intracellular localization of pVP2 and HA was determined by an indirect immunofluorescence assay using α-VP2 and α-HA antibodies (Fig. 4B). The pVP2 protein was detected in clusters dispersed throughout the cytoplasm, and only in SDS-permeabilized cells, whereas HA could be detected both in the presence and absence of SDS. This indicates that the pVP2 protein remained inside the cells and that the HA protein was displayed on the outside of the plasma membrane, as expected. To investigate whether the viral (glyco)proteins showed the correct molecular mass and whether HA was glycosylated, cell lysates of replicon RNA-transfected BHK-21 cells were analyzed on a western blot (Fig. 4C-E). The pVP2 protein migrated at the expected molecular mass of ~48 kDa (Fig. 4C). An additional faint band of 55 kDa was observed, which could result from incomplete ribosome skipping by FMDV-2A (Fig. 4A) [11,39].

For the detection of HA glycosylation, the cell lysates of transfected cells with either the TMUV or VEEV replicon RNA were treated with peptide-N-glycosidase F (PNGase F) to remove putative *N*-linked oligosaccharides (Fig. 4D). The expression of HA from either replicon RNAs was detected at a molecular mass of ~70-100 kDa. In the PNGase F-treated samples, both detected protein bands shifted to a single protein band at a molecular mass of ~60 kDa, suggesting that HA was indeed *N*-glycosylated. To confirm the tethering of the HA protein in the plasma membrane, the (concentrated) supernatant was screened for the presence of any soluble HA protein (Fig. 4E), which confirmed that no HA protein could be detected in the supernatant.

3.4. Formulation of DREP and replicon RNA into lipid nanoparticles (LNPs)

Replicon RNA or DREP was formulated in LNPs for the *in vivo* delivery to chickens. Both VEEV and TMUV replicon RNAs and DREPs were purified and formulated using the NanoAssemblr Ignite microfluidic system to mix an organic phase of lipids in ethanol with an aqueous phase containing the nucleic acids into LNPs (Fig. 5A). These LNPs were then analyzed using transmission electron microscopy (TEM) and dynamic light scattering (DLS) to characterize the LNP shape and size (Fig. 5B-5D). Particles were detected ranging from 50 to 600 nm in diameter (Fig. 5B). Although no significant difference was detected in the mean particle size between the various formulations, LNPs sized larger than 300 nm were only observed when LNPs contained a nucleic acid cargo (Fig. 5C). The analysis of LNPs using DLS yielded an average size of 150 nm with a similar diversity in particle size and a comparable trend in size distribution as for empty LNPs (Fig. 5D). For 1-day-old chickens to be vaccinated with 10 μg or 3 μg of LNP:RNA or LNP:DREP, respectively, a minimal concentration of 50 ng/μL formulated vaccine should be achieved to minimize the injection volume. To accurately determine the vaccination dose and quality of the formulated replicon RNA, an LNP:RNA disruption assay was performed (Fig. 5E). This assay showed that a concentration of 94–140 ng of replicon RNA/μL of the formulated vaccine was realized and that the quality of replicon RNA was similar to before the formulation. Furthermore, it was shown

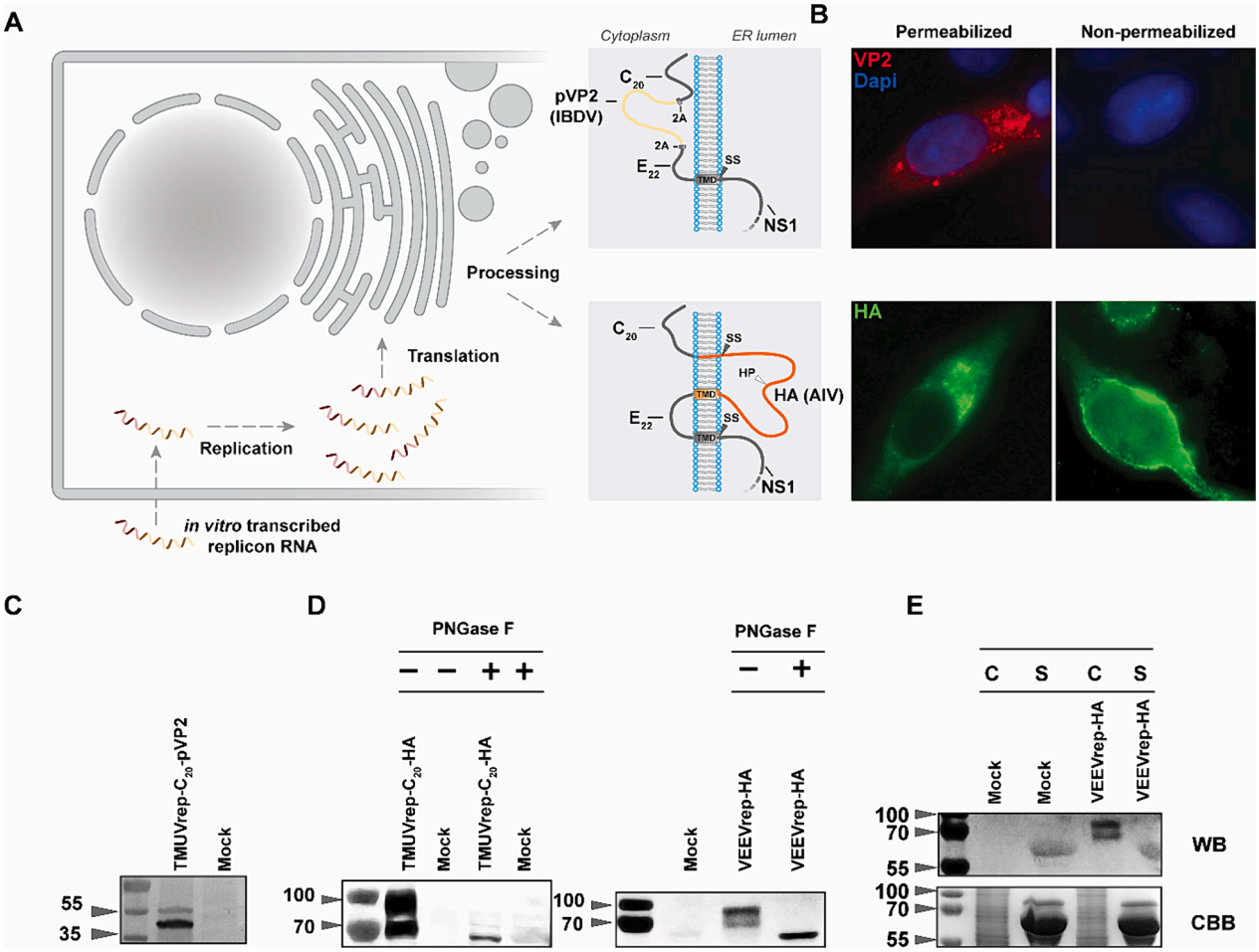

Fig. 4. Cellular location and processing of viral (glyco)proteins expressed using replicon RNA in BHK-21 cells. (A) A schematic overview of the replication and translation of *in vitro* transcribed replicon RNA and the membrane topology of the viral (glyco)proteins in the cytoplasm or the lumen of the endoplasmic reticulum (ER). C20: first 20 amino acids of capsid (C) protein, E22: last 22 amino acids of envelope (E) protein, 2A: foot-and-mouth disease virus element 2A, HP: trypsin-like protease cleavage site, SS: signal peptide cleavage sites, TMD: *trans*-membrane domain, NS1: viral non-structural protein 1. (B) Indirect immunofluorescence assay of transfected BHK-21 cell in the presence (left) or absence (right) of 0.1% SDS for the localization of viral (glyco)proteins. (C) Western blot analysis of transfected BHK-21 cell lysate for the detection of pVP2. (D) Lysate from BHK-21 cells transfected with TMUV replicon RNA (left) or VEEV replicon RNA (right) were analyzed using western blot for the presence of *N*-glycosylation of HA (E) Western blot (WB; top panel) and Coomassie brilliant Blue (CBB; bottom panel) of HA detection in both the cellular fraction (*c*) and concentrated supernatant (*s*) of transfected BHK-21 cells. Primary antibodies: α-HA convalescent chicken sera and monoclonal α-VP2 IgG (mouse). Secondary antibodies for immunofluorescence assay: Alexa Fluor 488 or 546-conjugated α-chicken IgY (goat) or α-mouse IgG (goat) respectively. Secondary antibodies for western blot: alkaline phosphatase-conjugated α-chicken IgY (goat) or α-mouse IgG (goat). Cell nuclei were counterstained using Hoechst. Protein sizes in kDa are indicated on the left.

that a formulation efficiency of more than 50 % was obtained in all formulations (Table 1).

3.5. RNA replicon and DREP vaccination of chickens against IBDV

To test the ability of TMUV replicons to induce an antigen-specific immune response in chickens, the LNP:RNA and LNP:DREP formulations encoding either HA (Fig. 6) or pVP2 (Figs. 7 and 8) were used in a prime-boost vaccination study. Each experimental group consisted of ten chickens, while the unvaccinated (mock) group include five chickens. At T = 0 weeks, prime vaccination with 10 μg of LNP:RNA or 3 μg LNP:DREP encoding the HA protein was conducted by injection into the right leg of day-old chickens. At T = 3 weeks, a booster injection of 10 μg or 3 μg was administered, respectively (Fig. 6A). Serum was obtained at timepoints T = 3, 5, and 7 weeks post prime vaccination (ppv), and the antibody response was detected by reversed competition ELISA, indirect ELISA (Fig. 6B–E), or hemagglutinin inhibition assay (Supplementary Fig. S3). In all the sera and at all time points, no significant response against HA passed the manufacturer's threshold for seroconversion in the reversed competition ELISA, irrespective of whether the chickens were vaccinated with TMUV or VEEV replicon RNA (Fig. 6B). Only one chicken in the group vaccinated with VEEVrep-H5 replicon RNA showed a positive seroconversion in the reversed competition ELISA (Fig. 6B) and a positive response in the HI test (Supplementary Fig. S3) at 7 weeks post-prime vaccination. Similar to the reversed competition assay, no significant HA-specific antibody response was detected in the sera of TMUV replicon RNA vaccinated chickens using an indirect ELISA (Fig. 6C). Only at T = 7, the detection level of α-HA antibodies in the VEEV replicon RNA-vaccinated group was significantly higher than for the mock group.

Chickens were also vaccinated with DREP:LNP formulations. In this experiment, immunization with TMUV DREP did not results in a detectable antibody response, as determined by the reversed competition ELISA nor the indirect ELISA, (Fig. 6D & E). In contrast, the VEEV DREP vaccinated chickens showed the initiation of seroconversion in the reversed competition ELISA after a single vaccination at T = 3 weeks, while a significant difference in HA titers in the indirect ELISA was detected after booster administration at T = 5 weeks (Fig. 6D & E).

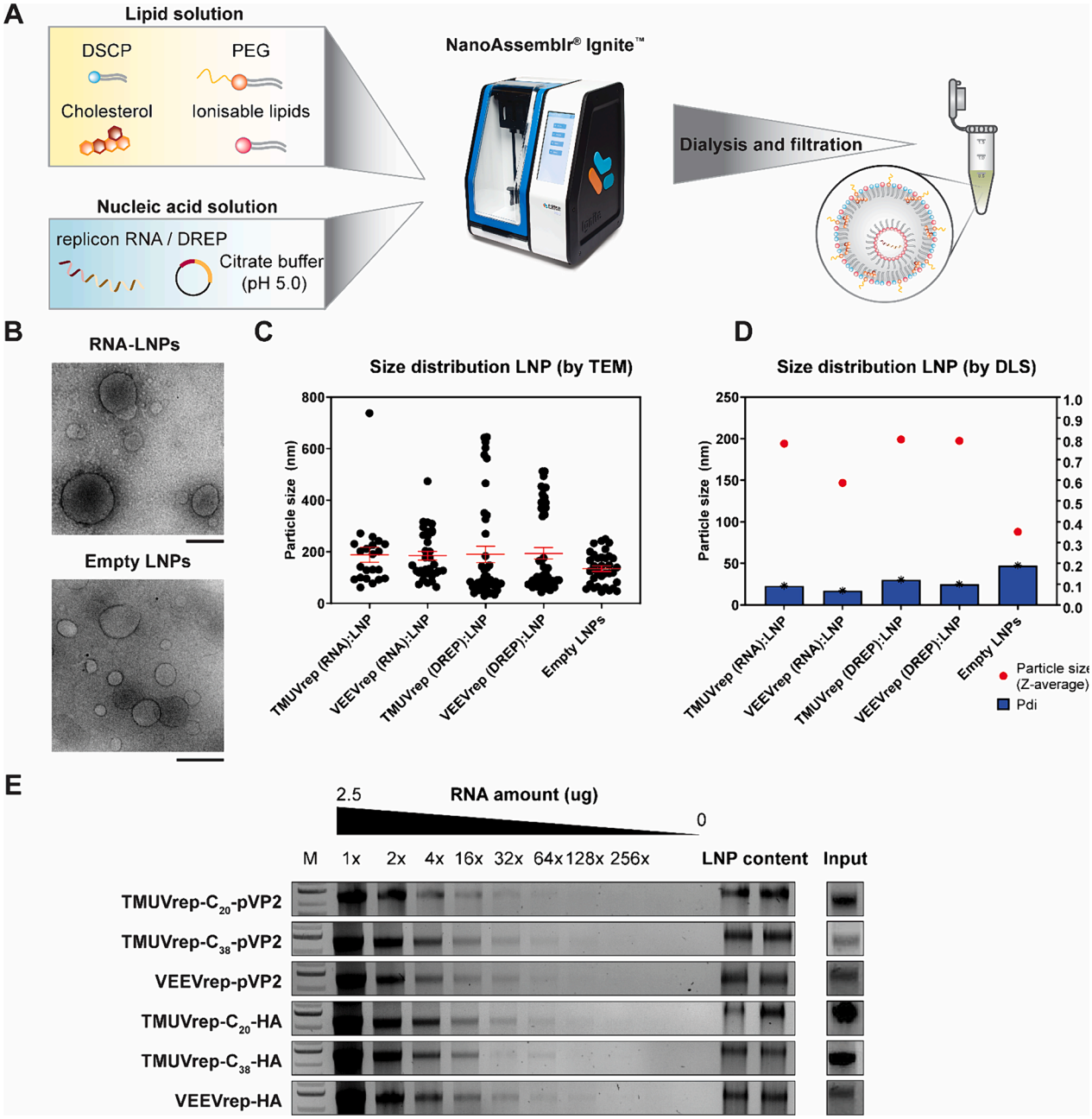

Fig. 5. Replicon RNA and DREP formulation in lipid nanoparticles (LNPs). (A) Schematic overview of the formulation of lipid nanoparticles (LNPs) using the NanoAssemblr Ignite microfluidic system by mixing an aqueous phase, containing replicon RNA in a citrate buffer (pH 5) and an organic phase, containing ionisable lipids, cholesterol, distearoylphosphatidylcholine (DSCP), and polyethylene glycol (PEG). (B) Empty and RNA-containing LNPs were analyzed by transmission electron microscopy (TEM) and the size distribution determined via (C) semiquantitative analysis from the acquired TEM images or (D) dynamic light scattering (DLS). For the measurements using DLS, the average particle size (Z-average; left axis) and size polydispersity index (Pdi; right axis) were visualized in the graph. (E) An LNP disruption assay was performed to determine the quantity and quality of the formulated LNPs against a replicon RNA standard visualized via conventional gel electrophoresis. The dilution factors of the RNA standard (1x-256x) are indicated above the images. 'Input' resembles unpurified, unformulated *in vitro*-transcribed RNA. Error bars represent standard error. Scale bars represent 200 nm.

Another immunization trial was performed to test the function of the TMUV in comparison to VEEV replicons in eliciting an immune response against VP2 (IBDV). Sample groups were set up similarly as for the HA study, except that the positive control was immunized using Innovax-ND-IBD® (MSD Animal Health). At T = 0 weeks, the prime vaccination of 10 µg of LNP:RNA (Fig. 7) or 3 µg LNP:DREP (Fig. 8) was injected into the right leg of day-old chickens. At T = 3 weeks ppv, an additional booster injection (10 µg for LNP:RNAs or 3 µg for LNP:DREPs) was administered (Figs. 7A or 8A). Following this prime vaccination, no significant increase in antibody titers was detected at 3 weeks ppv (T = 3 weeks) with LNP:RNA (Fig. 7B, C). However, two weeks after the booster vaccination (T = 5 weeks) seroconversion was detected in both TMUVrep-C_{20}-pVP2 and TMUVrep-C_{38}-pVP2 vaccinated groups, which clearly differed from the VEEVrep-pVP2 vaccinated group ($p \leq 0.05$) which showed no humoral immune response at this time point. Unfortunately, due to a technical failure in two isolators, 80 % of the chickens assigned to the positive control group and 100 % of chickens assigned to the TMUVrep-C_{20}-VP2 replicon RNA group were lost during this experiment. No significant virus neutralization titers were observed in any of the experimental groups at 5 or 13 weeks post vaccination, in

Table 1
Formulation efficiency of the replicon RNA formulation in lipid nanoparticles (LNPs).

	Input (mg)	Concentration RNA in LNP (ng/µl)	Total volume LNP formulation (mL)	Total RNA LNP formulation (mg)	Encapsidation efficiency (%)
HA encoding replicons					
TMUVrep-C_{20}-HA	0.75	108	3.5	0.38	50.5
TMUVrep-C_{38}-HA	0.68	94	4	0.38	55.0
VEEVrep-HA	0.82	138	4	0.55	67.5
pVP2 encoding replicons					
TMUVrep-C_{20}-pVP2	0.75	140	4	0.56	74.6
TMUVrep-C_{38}-pVP2	0.73	129	4	0.52	70.7
VEEVrep-pVP2	0.75	132	4	0.53	70.6

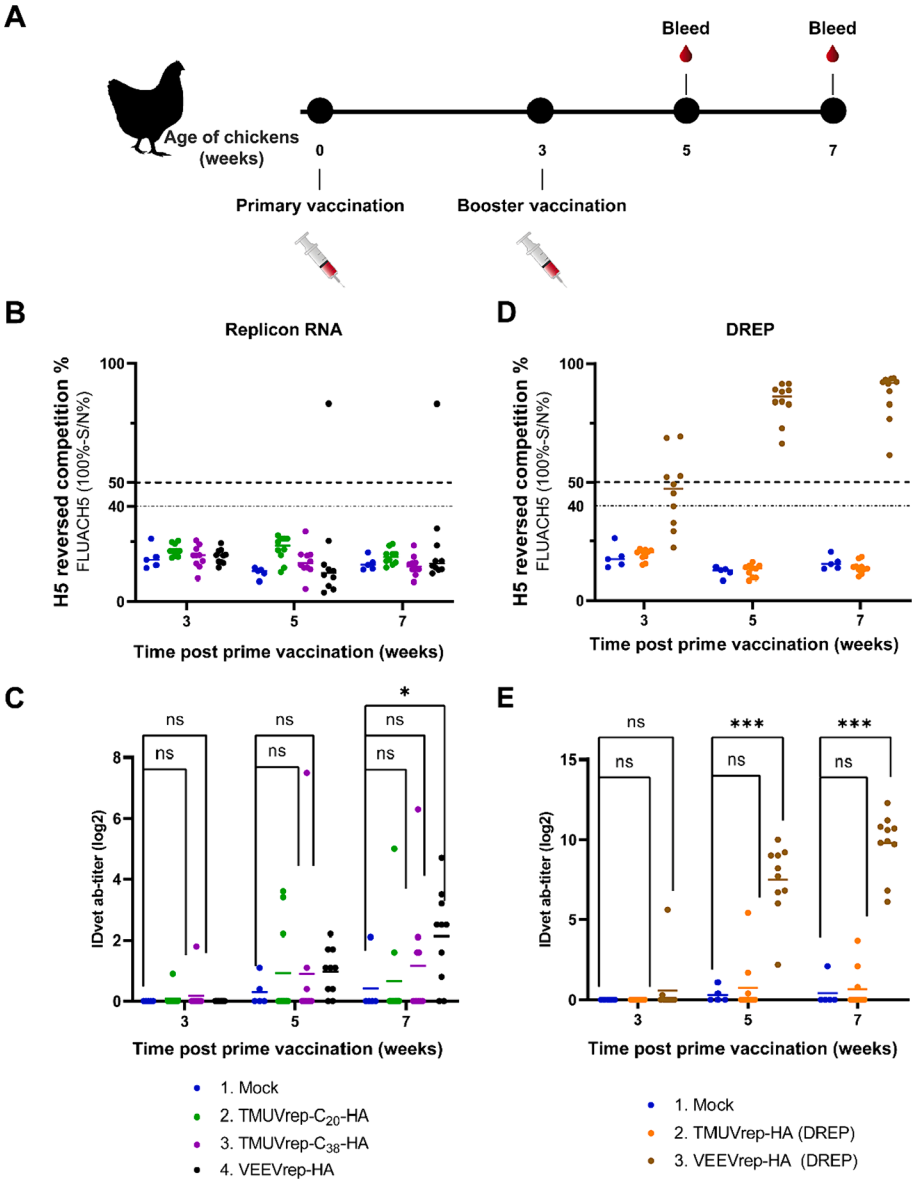

Fig. 6. Immunogenicity of SPF-chickens using LNP-formulated replicon RNAs (left) and DREPs (right) expressing HA (AIV) antigen. (A) Timeline of immunization and key points (B) Competitive and (C) indirect ELISA assay detecting the presence of anti-HA in the serum of replicon RNA vaccinated chickens. (D) Competitive and (E) indirect ELISA assay detecting the presence of anti-HA in the serum of DREP vaccinated chickens. Dotted lines in the competitive ELISA graphs (40–50 %) correspond with a "uncertain" competition percentage (100 %-S/N%) according to the manufacturers protocol. Data equal or above 50 % are considered positive while data equal or less than 40 % are considered negative. Statistical significance was determined compared to the mock group using the Mann-Whitney *U* test (* = $p \leq 0.05$, ** = $p \leq 0.01$ *** = $p \leq 0.001$, **** = $p \leq 0.0001$, ns = no significant difference).

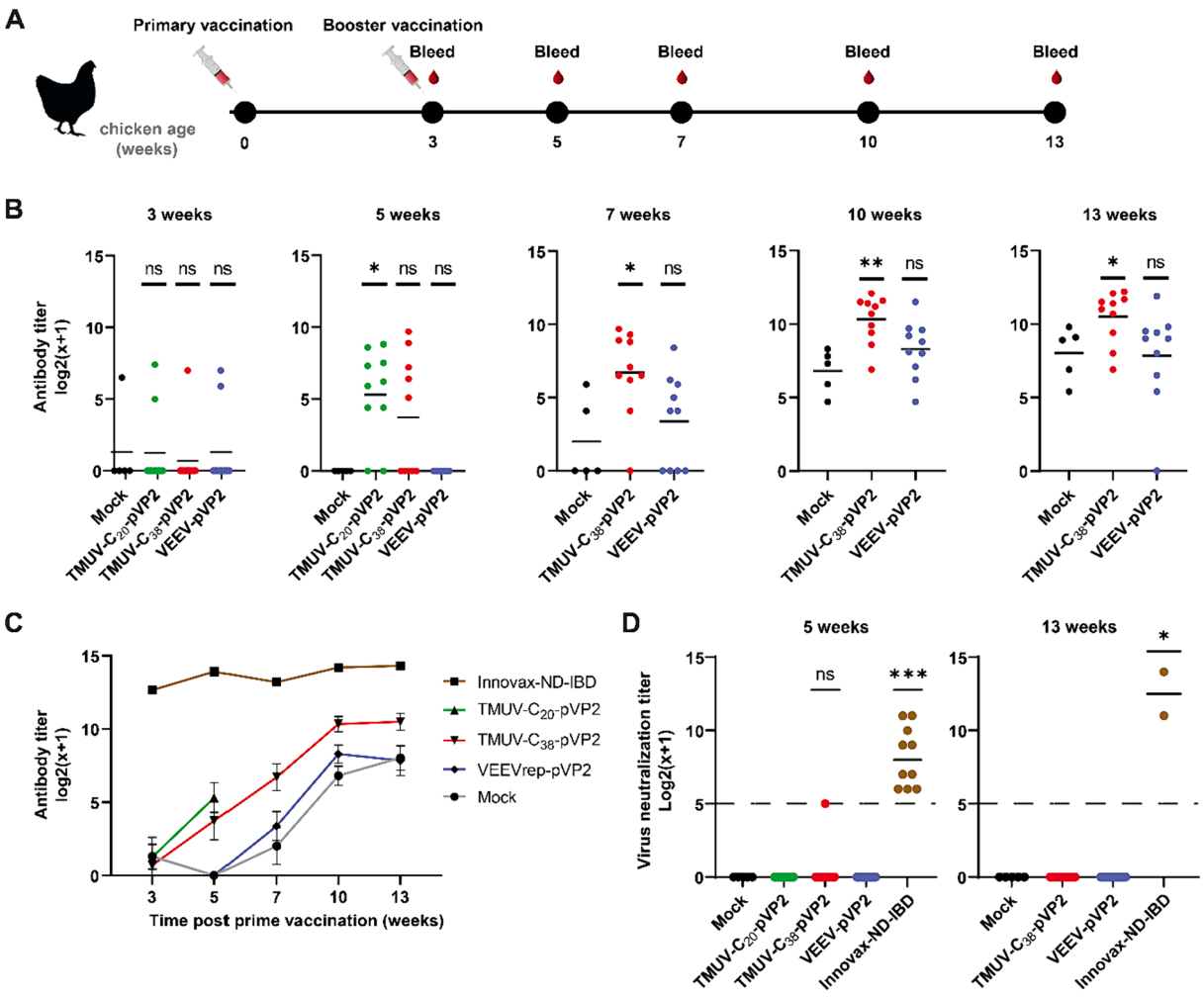

Fig. 7. Immunogenicity of SPF-chickens vaccinated using LNP-formulated replicon RNAs expressing pVP2 (IBDV) antigen. (A) Timeline of immunizations and key points (B-C) Indirect ELISA detecting α-VP2 antibodies in groups vaccinated with Innovax-ND-IBD® (brown), TMUVrep-C_{20}-pVP2 (green), TMUVrep-C_{38}-pVP2 (red), VEEVrep-pVP2 in (blue), mock (black). (D) Virus neutralization titers using IBDV strain D78 and chicken embryonic cells. Statistical significance was determined compared to the mock group using the Mann-Whitney *U* test (* = $p \leq 0.05$, ** = $p \leq 0.01$, ns = no significant difference).

contrast to the positive control group (Fig. 7D).

For the LNP:DREP-vaccinated chickens a different response profile was observed. The presence of antibodies in VEEVrep-pVP2 DREP-vaccinated chickens was detected as early as 3 weeks post-prime vaccination (T = 3 weeks; Fig. 8B, C). Although neither was significantly different from the mock ($p = 0.178$), a noticeably higher antibody titer was detected in the VEEVrep-pVP2 DREP-vaccinated group compared to the TMUVrep-pVP2 DREP-vaccinated group ($p = 0.0325$) at T = 3 weeks. Following the booster vaccination, a progressive increase in antibody titers was observed in VEEVrep-pVP2 DREP-vaccinated chickens for up to 13 weeks post-prime vaccination, approaching the antibody titers observed in the positive control group. This group also had high virus neutralization titers at 13 weeks post immunization (Fig. 8D). In contrast, TMUV DREP-vaccinated chickens demonstrated a slower but still significant difference in α-VP2 antibody titers starting from ten weeks post-prime vaccination (T = 10 weeks), although no virus-neutralizing activity was measured (Fig. 8D). Throughout the VP2 immunization trial, an overall increase in antibody titer readouts was observed for all groups and was particularly notable in mock, VEEVrep-pVP2 replicon RNA- and VEEVrep-pVP2 (DREP)-vaccinated groups. This increase often coincided with the rise in plasma viscosity as the chickens aged also resulting in a higher background [47].

4. Discussion

In the wake of the success of mRNA vaccination, self-amplifying mRNA or replicon vaccines are gaining renewed attention as a highly versatile and safe vaccination alternative for a range of animal species. It has been demonstrated that the well-studied VEEV replicon platform provided protective immunity against SARS-CoV-2 or Rabies virus in mice [29,67]; Ebolavirus in non-human primates [19]; and Influenza A virus or PEDV in swine [6,10]. However, the VEEV-based replicon vaccine underperformed in mounting a protective immune response in young chickens [50]. In our research, our aim was to develop a bird-adapted TMUV replicon platform that induced a potent antibody response against common poultry infections such as AIV and IBDV. We demonstrated that TMUV RNA replicons as well as DNA-launched replicons can be successfully used to express reporter and viral antigens *in vitro* (Fig. 1). Notably, while VEEVrep-Rluc replicon RNA demonstrated an earlier onset of heterologous gene expression and high levels of Rluc activity in the first 24 hpe, the overall Rluc expression was significantly higher for the TMUVrep-C_{20}-Rluc replicon RNA. This can be attributed to the higher cytopathic effect induced by the VEEVrep-Rluc replicon RNA resulting from the expression activity of the 26S subgenomic promoter of VEEV [12,14,44,48,61]. The inclusion of the DCS-PK in the TMUV replicon likely contributed to the earlier onset of transgene expression for the TMUVrep-C_{38}-GFP replicon RNA but also to

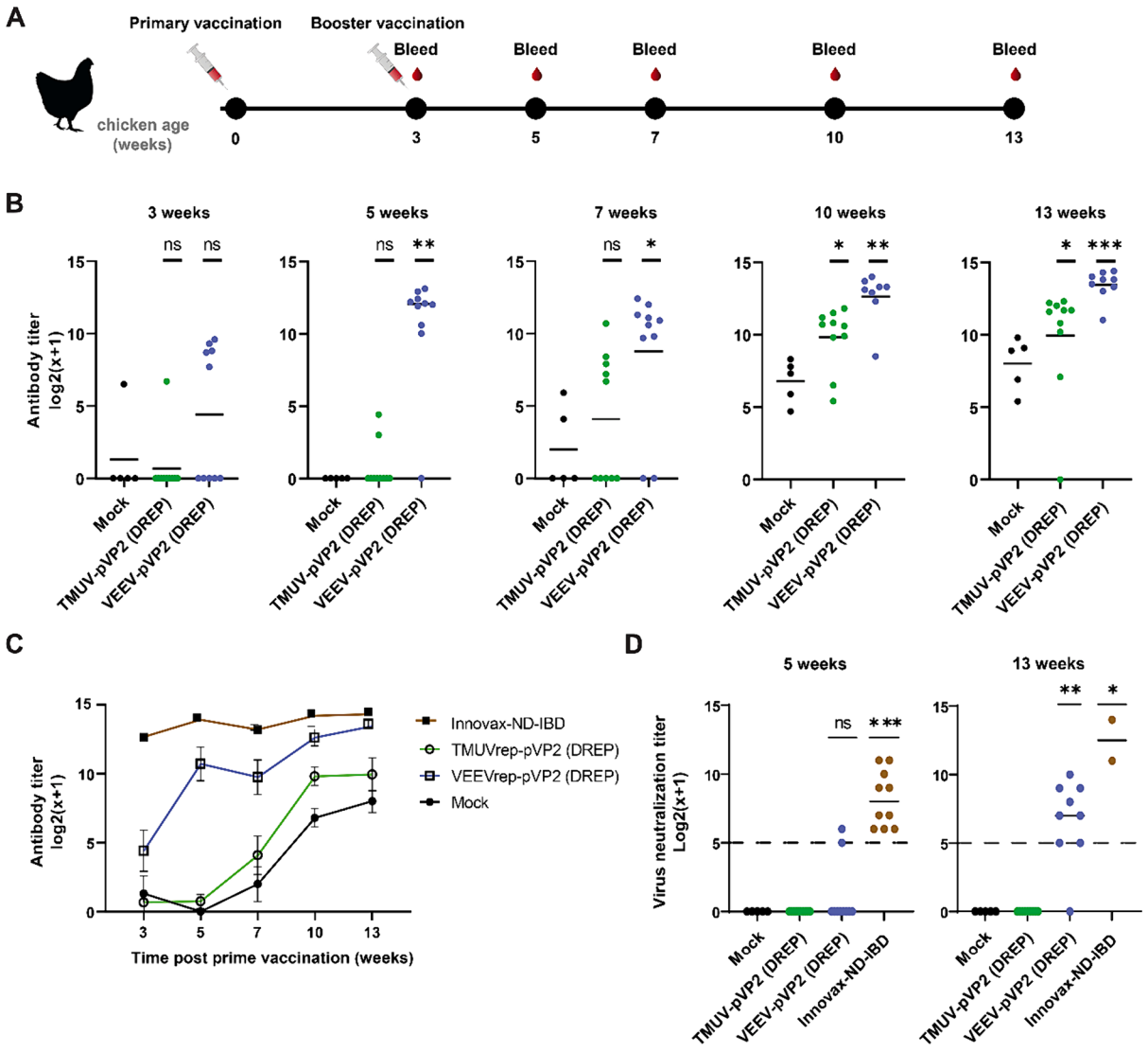

Fig. 8. Immunogenicity of SPF-chickens vaccinated using LNP-formulated DREPs expressing pVP2 (IBDV) antigen. (A) Timeline of immunizations and key points (B-C) Indirect ELISA detecting α-VP2 IgY in chicken sera in groups vaccinated with Innovax-ND-IBD® (brown), TMUVrep-C_{20}-pVP2 DREP (green), VEEVrep-pVP2 in (blue), mock (black). (D) Virus neutralization titers using IBDV strain D78 and chicken embryonic cells. Statistical significance was determined compared to the mock group using the Mann-Whitney *U* test (* = $p \leq 0.05$, ** = $p \leq 0.01$). (* = $p \leq 0.05$, ** = $p \leq 0.01$ *** = $p \leq 0.001$, ns = no significant difference).

an increase in CPE (Fig. 2). The effects of replicon-induced CPE on vaccine efficacy are not easy to predict – on the one hand, CPE limits the duration of protein expression in antigen-expressing cells, but on the other hand, enhanced CPE may also lead to stimulation of innate immunity and attraction of immune cells [46,62,61]. However, at later time points, no notable difference in the overall GFP expression level of TMUVrep-C_{38}-GFP was observed compared to TMUVrep-C_{20}-GFP replicon RNA, as was also reported for another TMUV replicon system [18]. These findings highlight the flexibility of the TMUV replicon system in tuning the expression of heterologous proteins and the induction of CPE.

For the expression of pVP2 of IBDV, the FMDV-2A ribosomal skipping elements released the pVP2 from the TMUV polyprotein and demonstrated a molecular mass and intracellular localization in line with what has been described for a wildtype IBDV infection [4,24,35]. The AIV HA expressed from the TMUV replicon was displayed on the plasma membrane similar to other heterologously expressed HA proteins [22] (Figs. 3 and 4). Immunoblotting of the cell lysate showed two distinct protein bands at ~70 and ~100 kDa. Heterogeneity in glycosylation patterns and protein processing have been observed amongst HA proteins [7,27]; C. [30], suggesting that HA is *N*-glycosylated similar to a wildtype avian influenza infection [40].

After successful *in vitro* expression of viral (glyco)proteins, the formulation of both replicon modalities (RNA and DREP constructs of TMUV and VEEV) in LNPs was performed in preparation for the animal study (Fig. 5). The formulated LNPs displayed a variable size ranging from small (~30 nm) to very large (~700 nm) measured via digital image analysis and DLS. Although DLS is used to measure the hydrodynamic radius and not the actual particle size, it should be noted that size variation was expected between both measuring techniques. Additionally, the analyses only provided a snapshot of the current size homogeneity of the LNPs while these might have temporal dynamics or be affected by the sample preparation for analysis [25]. The understanding of the impact of LNP particle size is reported to be an important parameter for enabling potent LNP vaccines. A study in mice reporting an average particle size of around 100 nm was ideal for the consistent production of high antibody titers [16]. Since this is the first study considering LNP-formulated RNA or DNA in chickens, further validation of the optimal size homogeneity of the LNPs should be performed. Optimizing the RNA:LNP ratios or the relative composition of the

different lipids may help to reduce LNP size heterogeneity.

We demonstrated that a prime-boost vaccination trial in SPF layers using LNP-formulated TMUV replicon RNA induced higher antibody titers against the pVP2 of IBDV than for VEEV replicon RNA expressing the same antigen. It might be that the slower but robust transgene expression in addition to the minimal CPE of the TMUV replicon RNA *in vitro,* contributes to a more sustained response in chickens compared to the VEEV replicon RNA [14,18,46]. Notably, TMUVrep-C_{38}-pVP2 was significantly different from the mock from 7 weeks until the end of the study (13 weeks), whereas VEEV replicon RNA was not. Interestingly, TMUVrep-C_{20}-pVP2 was already significant at week 5, suggesting that both TMUV replicon variants outperformed VEEV replicon in this animal trial (Fig. 7).

In contrast to the successful induction of IBDV VP2-specific antibodies in the HA study, neither TMUV nor VEEV replicon RNA vaccinated groups showed significant induction of HA-specific antibodies in both reversed competition and indirect ELISA at week 3 and 5 ppv (Fig. 6). Despite this, a few individual responders in the replicon RNA vaccinated groups showed the first indication of seroconversion at week 3, but only the VEEV replicon RNA vaccinated group showed significant induction of HA-specific antibodies at week 7. Whether these low antibody titers confer protection during a homologous or heterologous challenge remains to be tested in future studies. Since no studies have been performed with LNP-formulated replicon RNA in chickens, it is still unresolved if the induction of α-HA antibodies requires a higher dose or longer incubation times before seroconversion is observed. Different studies tested the administration of various LNP-formulated replicon RNA doses ranging from 0.5 $\mu g kg^{-1}$ to 500 $\mu g kg^{-1}$ [13,36,37]. This is in line with the estimated 200 $\mu g kg^{-1}$ RNA dose in the current study. However, it should be noted that these studies only evaluated the delivery of VEEV replicon RNA in mice and not in chickens.

A notable observation was that VEEV DREP in both the pVP2 and HA studies showed an early onset (T = 3) of antibody response after a single vaccination (Figs. 6 and 8). Intriguingly, the VEEV DREP vaccinated group in the HA study even outcompeted the positive control at week 7, while the HVT-vectored vaccines used to immunize chickens maintain the ability to spread from cell to cell and therefore persist much longer than most RNA and DNA vaccines[23]. In contrast to the VEEV DREP, the TMUV-based DREP only induced a significant response in the pVP2 study after the administration of the booster. Further, only the VEEV DREP immunization induced a virus-neutralizing antibody response against IBDV, which was in accordance with the ELISA readout. Whether the slower seroconversion of the TMUV DREP vaccinated animals could be explained with the inherent different expression kinetics compared to VEEV replicon remains untested.

Another reason why the constructed TMUV DREP efficacy tested both *in vitro* as well as *in vivo* differs compared to the VEEV DREP, could be explained by the difference in molar mass between the constructs (TMUV DREP = 13.6×10^6 $g mol^{-1}$ vs VEEV DREP = 7.8×10^6 $g mol^{-1}$). In this study, only 3 μg of DREP was administered in each dose without considering the normalization for the DREP size. This would mean that the TMUV DREP dose per chicken is 43 % less than for VEEV DREP-vaccinated chickens. Whether DREP vaccination in general, conveys a longer protection compared to replicon RNA has not been evaluated, but it is known that conventional plasmid DNA as well as replicon-encoding DNA plasmids can be maintained in cells for months [14,42,45]. Furthermore, it was expected that from both replicon modalities, the replicon RNA might show an earlier onset of antigen production than its DNA counterpart. The required nuclear delivery to initiate RNA transcription compared to the direct translation of *in vitro* transcribed replicon RNA in the cytoplasm, might explain the delayed generation of an antibody response of TMUV DREP compared to the TMUV replicon RNA in the IBDV vaccination study.

A limitation of our study is that we analyzed humoral, but not cellular, immunity in the chicken vaccination trials with different replicon modalities (RNA and DNA). Therefore, performing an optimal dose finding in combination with a virus challenge study would be critical to identify the requirements to elicit a protective immune response in chickens using these self-amplifying mRNA vaccine platforms.

Funding

Funded by MSD Animal Health. Funders had no role in the decision to publish. Funders conducted the LNP-formulations and animal trials.

CRediT authorship contribution statement

Jerome D.G. Comes: . **Kristel Doets:** Data curation, Formal analysis, Investigation, Methodology. **Thijmen Zegers:** Data curation, Formal analysis, Investigation, Methodology. **Merel Kessler:** Data curation, Formal analysis, Investigation, Methodology. **Irene Slits:** Data curation, Formal analysis, Investigation, Methodology. **Natalia A. Ballesteros:** Formal analysis, Methodology, Validation. **Noortje M.P. van de Weem:** . **Henk Pouwels:** Formal analysis, Methodology, Validation. **Monique M. van Oers:** Supervision, Writing – review & editing. **Marielle C.W. van Hulten:** Conceptualization, Supervision. **Martijn Langereis:** Investigation, Supervision, Writing – review & editing. **Gorben P. Pijlman:** Conceptualization, Funding acquisition, Supervision, Writing – review & editing.

Declaration of competing interest

The authors declare the following financial interests/personal relationships which may be considered as potential competing interests: Gorben Pijlman reports financial support was provided by MSD Animal Health. Martijn Langereis, Noortje van de Weem, Henk Pouwels, Natalia Ballesteros reports a relationship with MSD Animal Health that includes: employment. If there are other authors, they declare that they have no known competing financial interests or personal relationships that could have appeared to influence the work reported in this paper.

Data availability

No data was used for the research described in the article.

Acknowledgments

The authors are thankful to Jelmer Vroom from the Wageningen Electron Microscopy Centre for the electron microscopy analysis of LNPs and Marleen Henkens, Corinne Geertsema, Frans Manders, Christiaan Vossen, and Martin Piest for their technical assistance. We thank Mateusz Walczak, Linda van Oosten, Tessy Hick, and Jelke Fros for their helpful discussions. The RepliCAID project was funded by MSD Animal Health.

Appendix A. Supplementary data

Supplementary data to this article can be found online at https://doi.org/10.1016/j.vaccine.2024.03.032.

References

[1] Baz M, Luke CJ, Cheng X, Jin H, Subbarao K. H5N1 vaccines in humans. Virus Res 2013;178(1):78–98.
[2] Bloom K, van den Berg F, Arbuthnot P. Self-amplifying RNA vaccines for infectious diseases. Gene Ther 2021;28(3–4):117–29.
[3] Chen H, Bu Z. Development and application of avian influenza vaccines in China. In: Compans RW, Orenstein WA, editors. Vaccines for Pandemic Influenza, Vol. 333. Berlin Heidelberg: Springer; 2009. p. 153–62.
[4] Chevalier C, Lepault J, Erk I, Da Costa B, Delmas B. The maturation process of pVP2 requires assembly of infectious bursal disease virus capsids. J Virol 2002;76(5):2384–92.

[5] Comes JDG, Poniman M, van Oosten L, Doets K, de Cloe S, Geertsema C, et al. Infectious clone of a contemporary Tembusu virus and replicons expressing reporter genes or heterologous antigens from poultry viruses. Biotechnol J 2023; e2300254.
[6] Crawford K, Lager KM, Kulshreshtha V, Miller LC, Faaberg KS. Status of vaccines for porcine epidemic diarrhea virus in the United States and Canada. Virus Res 2016;226:108–16.
[7] Cruz E, Cain J, Crossett B, Kayser V. Site-specific glycosylation profile of influenza A (H1N1) hemagglutinin through tandem mass spectrometry. Hum Vaccin Immunother 2018;14(3):508–17.
[8] Darty K, Denise A, Ponty Y. VARNA: Interactive drawing and editing of the RNA secondary structure. Bioinformatics 2009;25(15):1974–5.
[9] Erasmus JH, Khandhar AP, O'Connor MA, Walls AC, Hemann EA, Murapa P, et al. An alphavirus-derived replicon RNA vaccine induces SARS-CoV-2 neutralizing antibody and T cell responses in mice and nonhuman primates. Sci Transl Med 2020;12(555):eabc9396.
[10] Erdman MM, Kamrud KI, Harris DL, Smith J. Alphavirus replicon particle vaccines developed for use in humans induce high levels of antibodies to influenza virus hemagglutinin in swine: Proof of concept. Vaccine 2010;28(3):594–6.
[11] Furler S, Paterna J-C, Weibel M, Büeler H. Recombinant AAV vectors containing the foot and mouth disease virus 2A sequence confer efficient bicistronic gene expression in cultured cells and rat substantia nigra neurons. Gene Ther 2001;8 (11):864–73.
[12] Garmashova N, Gorchakov R, Volkova E, Paessler S, Frolova E, Frolov I. The Old World and New World alphaviruses use different virus-specific proteins for induction of transcriptional shutoff. J Virol 2007;81(5):2472–84.
[13] Geall AJ, Verma A, Otten GR, Shaw CA, Hekele A, Banerjee K, et al. Nonviral delivery of self-amplifying RNA vaccines. Proc Natl Acad Sci 2012;109(36): 14604–9.
[14] Gehrke R, Heinz FX, Davis NL, Mandl CW. Heterologous gene expression by infectious and replicon vectors derived from tick-borne encephalitis virus and direct comparison of this flavivirus system with an alphavirus replicon. J Gen Virol 2005;86(4):1045–53.
[15] Hamel R, Phanitchat T, Wichit S, Morales Vargas RE, Jaroenpool J, Diagne CT, et al. New insights into the biology of the emerging Tembusu virus. Pathogens 2021;10(8):1010.
[16] Hassett KJ, Higgins J, Woods A, Levy B, Xia Y, Hsiao CJ, et al. Impact of lipid nanoparticle size on mRNA vaccine immunogenicity. J Control Release 2021;335: 237–46.
[17] Haveri A, Solastie A, Ekström N, Österlund P, Nohynek H, Nieminen T, et al. Neutralizing antibodies to SARS-CoV-2 Omicron variant after third mRNA vaccination in health care workers and elderly subjects. Eur J Immunol 2022;52 (5):816–24.
[18] He Y, Wang X, Guo J, Mao L, Zhang S, Hu T, et al. Replication/assembly defective avian flavivirus with internal deletions in the capsid can be used as an approach for living attenuated vaccine. Front Immunol 2021;12:694959.
[19] Herbert AS, Kuehne AI, Barth JF, Ortiz RA, Nichols DK, Zak SE, et al. Venezuelan equine encephalitis virus replicon particle vaccine protects nonhuman primates from intramuscular and aerosol challenge with ebolavirus. J Virol 2013;87(9): 4952–64.
[20] Homonnay ZG, Kovács EW, Bányai K, Albert M, Fehér E, Mató T, et al. Tembusu-like flavivirus (Perak virus) as the cause of neurological disease outbreaks in young Pekin ducks. Avian Pathol 2014;43(6):552–60.
[21] Hooper JW, Ferro AM, Golden JW, Silvera P, Dudek J, Alterson K, et al. Molecular smallpox vaccine delivered by alphavirus replicons elicits protective immunity in mice and non-human primates. Vaccine 2009;28(2):494–511.
[22] Hsu HL, Millet JK, Costello DA, Whittaker GR, Daniel S. Viral fusion efficacy of specific H3N2 influenza virus reassortant combinations at single-particle level. Sci Rep 2016;6.
[23] Ingrao F, Rauw F, van den Berg T, Lambrecht B. Characterization of two recombinant HVT-IBD vaccines by VP2 insert detection and cell-mediated immunity after vaccination of specific pathogen-free chickens. Avian Pathol J World Vet Poultry Assoc 2017;46(3):289–99.
[24] Irigoyen N, Castón JR, Rodríguez JF. Host proteolytic activity Is necessary for infectious bursal disease virus capsid protein assembly. J Biol Chem 2012;287(29): 24473–82.
[25] Jakubek ZJ, Chen S, Zaifman J, Tam YYC, Zou S. Lipid nanoparticle and liposome reference materials: Assessment of size homogeneity and long-term -70 °C and 4 °C storage stability. Langmuir: ACS J Surf Colloids 2023;39(7):2509–19.
[26] Khromykh AA, Meka H, Guyatt KJ, Westaway EG. Essential role of cyclization sequences in flavivirus RNA replication. J Virol 2001;75(14):6719–28.
[27] Koroleva M, Batarse F, Moritzky S, Henry C, Chaves F, Wilson P, et al. Heterologous viral protein interactions within licensed seasonal influenza virus vaccines. NPJ Vaccines 2020;5(1):1–10.
[28] Kumar S, Stecher G, Tamura K. MEGA7: Molecular evolutionary genetics analysis version 7.0 for bigger datasets. Mol Biol Evol 2016;33(7):1870–4.
[29] Langereis MA, Albulescu IC, Stammen-Vogelzangs J, Lambregts M, Stachura K, Miller S, et al. An alphavirus replicon-based vaccine expressing a stabilized Spike antigen induces protective immunity and prevents transmission of SARS-CoV-2 between cats. NPJ Vaccines 2021;6(1):122.
[30] Li C, Shao M, Cui X, Song Y, Li J, Yuan L, et al. Application of deglycosylation and electrophoresis to the quantification of influenza viral hemagglutinins facilitating the production of 2009 pandemic influenza (H1N1) vaccines at multiple manufacturing sites in China. Biologicals 2010;38(2):284–9.
[31] Li D, Aaskov J, Lott WB. Identification of a cryptic prokaryotic promoter within the cDNA encoding the 5′ end of dengue virus RNA genome. PLoS One 2011;6(3):1–9.
[32] Liu L, Wang T, Wang M, Tong Q, Sun Y, Pu J, et al. Recombinant turkey herpesvirus expressing H9 hemagglutinin providing protection against H9N2 avian influenza. Virology 2019;529:7–15.
[33] Liu Z-Y, Li X-F, Jiang T, Deng Y-Q, Zhao H, Wang H-J, et al. Novel *cis*-acting element within the capsid-coding region enhances flavivirus viral-RNA replication by regulating genome cyclization. J Virol 2013;87(12):6804–18.
[34] Marangon S, Busani L. The use of vaccination in poultry production. Rev Sci Tech Off Int Epiz 2006;26(1):265–74.
[35] Maraver A, Oña A, Abaitua F, González D, Clemente R, Ruiz-Díaz JA, et al. The oligomerization domain of VP3, the scaffolding protein of infectious bursal disease virus, plays a critical role in capsid assembly. J Virol 2003;77(11):6438–49.
[36] McKay PF, Hu K, Blakney AK, Samnuan K, Brown JC, Penn R, et al. Self-amplifying RNA SARS-CoV-2 lipid nanoparticle vaccine candidate induces high neutralizing antibody titers in mice. Nat Commun 2020;11(1):3523.
[37] Melo M, Porter E, Zhang Y, Silva M, Li N, Dobosh B, et al. Immunogenicity of RNA replicons encoding HIV Env immunogens designed for self-assembly into nanoparticles. Mol Ther 2019;27(12):2080–90.
[38] Méndez F, Romero N, Cubas LL, Delgui LR, Rodríguez D, Rodríguez JF. Non-lytic egression of infectious bursal disease virus (IBDV) particles from infected cells. PLoS One 2017;12(1).
[39] Minskaia E, Nicholson J, Ryan MD. Optimisation of the foot-and-mouth disease virus 2A co-expression system for biomedical applications. BMC Biotech 2013;13 (1):67.
[40] Mishin VP, Novikov D, Hayden FG, Gubareva LV. Effect of hemagglutinin glycosylation on influenza virus susceptibility to neuraminidase inhibitors. J Virol 2005;79(19):12416–24.
[41] Moraga-Llop F. Vaccination against COVID-19 from 6 months of age on. Completing the circle of prevention in paediatrics. Vacunas (English Edition) 2023; 24(2):84–7.
[42] Morris-Downes MM, Phenix KV, Smyth J, Sheahan BJ, Lileqvist S, Mooney DA, et al. Semliki Forest virus-based vaccines: persistence, distribution and pathological analysis in two animal systems. Vaccine 2001;19(15–16):1978–88.
[43] Nei M, Kumar S. Molecular Evolution and Phylogenetics. USA: Oxford University Press; 2000.
[44] Petrakova O, Volkova E, Gorchakov R, Paessler S, Kinney RM, Frolov I. Noncytopathic replication of Venezuelan equine encephalitis virus and eastern equine encephalitis virus replicons in mammalian cells. J Virol 2005;79(12): 7597–608.
[45] Pietschmann T, Lohmann V, Rutter G, Kurpanek K, Bartenschlager R. Characterization of cell lines carrying self-replicating hepatitis C virus RNAs. J Virol 2001;75(3):1252–64.
[46] Pijlman GP, Suhrbier A, Khromykh AA. Kunjin virus replicons: an RNA-based, non-cytopathic viral vector system for protein production, vaccine and gene therapy applications. Expert Opin Biol Ther 2006;6(2):135–45.
[47] Robertson GW, Maxwell MH. Plasma viscosity values and the relationship with age and sex in normal commercial broiler and layer strains of chickens. Br Poult Sci 1996;37(2):309–16.
[48] Schlesinger S, Dubensky TW. Alphavirus vectors for gene expression and vaccines. Curr Opin Biotechnol 1999;10(5):434–9.
[49] Schröder A, van Loon AA, Goovaerts D, Mundt E. Chimeras in noncoding regions between serotypes I and II of segment A of infectious bursal disease virus are viable and show pathogenic phenotype in chickens. J Gen Virol 2000;81(Pt 2):533–40.
[50] Schultz-Cherry S, Dybing JK, Davis NL, Williamson C, Suarez DL, Johnston R, et al. Influenza virus (A/HK/156/97) hemagglutinin expressed by an alphavirus replicon system protects chickens against lethal infection with Hong Kong-origin H5N1 viruses. Virology 2000;278(1):55–9.
[51] Shortridge KF. Avian influenza viruses in Hong Kong: zoonotic considerations. In: Schrijver SR, Koch G, editors. Avian Influenza - Prevention and Control, Vol. 1. Springer; 2005. p. 9–18.
[52] Śmietanka K, Tyborowska J, Olszewska-Tomczyk M, Domańska-Blicharz K, Minta Z, Rabalski L, et al. A recombinant turkey herpesvirus expressing F and HN genes of avian avulavirus-1 (AAvV-1) genotype VI confers cross-protection against challenge with virulent AAvV-1 genotypes IV and VII in chickens. Viruses 2019;11 (9):784.
[53] Snyder DB, Lana DP, Cho BR, Marquardt WW. Group and strain-specific neutralization sites of infectious bursal disease virus defined with monoclonal antibodies. Avian Dis 1988;32(3):527–34.
[54] Swayne DE. Impact of vaccines and vaccination on global control of avian influenza. Avian Dis 2012;56(4 SUPPL.1):818–28.
[55] Sylte MJ, Hubby B, Suarez DL. Influenza neuraminidase antibodies provide partial protection for chickens against high pathogenic avian influenza infection. Vaccine 2007;25(19):3763–72.
[56] Tang N, Zhang Y, Pedrera M, Chang P, Baigent S, Moffat K, et al. A simple and rapid approach to develop recombinant avian herpesvirus vectored vaccines using CRISPR/Cas9 system. Vaccine 2018;36(5):716–22.
[57] van der Velden MVW, Geisberger A, Dvorak T, Portsmouth D, Fritz R, Crowe BA, et al. Safety and immunogenicity of a vero cell culture-derived whole-virus H5N1 influenza vaccine in chronically ill and immunocompromised patients. Clin Vaccine Immunol 2014;21(6):867–76.
[58] van Hulten MCW, Cruz-Coy J, Gergen L, Pouwels H, ten Dam GB, Verstegen I, et al. Efficacy of a turkey herpesvirus double construct vaccine (HVT-ND-IBD) against challenge with different strains of Newcastle disease, infectious bursal disease and Marek's disease viruses. Avian Pathol 2021;50(1):18–30.
[59] Vander Veen R, Kamrud K, Mogler M, Loynachan AT, McVicker J, Berglund P, et al. Rapid development of an efficacious swine vaccine for novel H1N1. PLoS Curr 2009;1:RRN1123.

[60] Vander Veen RL, Loynachan AT, Mogler MA, Russell BJ, Harris DLH, Kamrud KI. Safety, immunogenicity, and efficacy of an alphavirus replicon-based swine influenza virus hemagglutinin vaccine. Vaccine 2012;30(11):1944–50.
[61] Varnavski AN, Khromykh AA. Noncytopathic flavivirus replicon RNA-based system for expression and delivery of heterologous genes. Virology 1999;255(2):366–75.
[62] Varnavski AN, Young PR, Khromykh AA. Stable high-level expression of heterologous genes in vitro and in vivo by noncytopathic DNA-based Kunjin virus replicon vectors. J Virol 2000;74(9):4394–403.
[63] Wu D, Zou S, Bai T, Li J, Zhao X, Yang L, et al. Poultry farms as a source of avian influenza A (H7N9) virus reassortment and human infection. Sci Rep 2015;5:7630.
[64] Yee KS, Carpenter TE, Cardona CJ. Epidemiology of H5N1 avian influenza. Comp Immunol Microbiol Infect Dis 2009;32(4):325–40.
[65] Zai X, Shi B, Shao H, Qian K, Ye J, Yao Y, et al. Identification of a novel insertion site HVT-005/006 for the generation of recombinant turkey herpesvirus vector. Front Microbiol 2022;13:886873.
[66] Zeng X, Tian G, Shi J, Deng G, Li C, Chen H. Vaccination of poultry successfully eliminated human infection with H7N9 virus in China. Sci China Life Sci 2018;61(12):1465–73.
[67] Zhang H, Penninger JM, Li Y, Zhong N, Slutsky AS. Angiotensin-converting enzyme 2 (ACE2) as a SARS-CoV-2 receptor: molecular mechanisms and potential therapeutic target. Intensive Care Med 2020;2.